

# A comparison between the use of a high-resolution CCD camera and 35 mm film for obtaining coloured micrographs

A. ENTWISTLE

*The Ludwig Institute for Cancer Research, 91 Riding House Street, London W1P 8BT, U.K.*

**Key words.** Colour CCD camera, colour film, contrast light microscopy, resolution.

## Summary

In light microscopy, colour CCD cameras are now capable of generating image data sets that contain more information than can be captured with slow 35 mm colour reversal film. The resolution of colour CCD cameras with a high density of sensor elements ( $\geq 3300 \times 2200$  per channel of colour) is equivalent to that of slow 35 mm colour film over typical fields of view for objectives with a wide range of magnifications and numerical apertures. The contrast that can be achieved in images derived from the data sets obtained with colour CCD cameras far exceeds that found with film and can exceed that of human vision. Finally, the data sets collected with high-resolution colour CCD cameras are capable of being displayed at a wide range (four-fold) of different magnifications easily and interchangeably. Consequently, the combination of a data set that describes a relatively large field of view with one or two data sets that describe specific details taken with an eight-fold increase in magnification are all that is necessary to describe the salient features of the vast majority of stained specimens examined with transmitted light microscopy.

## Introduction

High quality colour photomicrographs can be difficult to produce. The effects of uneven illumination, unexpected reflections, lack of focus, out-of-focus blur, dirt and the imaging of suboptimal fields of view are only apparent hours to days after the film is exposed. Moreover, human visual perception is both highly efficient at filtering out such defects when observations are being made directly through a microscope and highly critical of the same defects when they appear in photomicrographs. Colour film is, however, capable of capturing all the spatial information that is available in the field of view of a microscope which has diffraction limited optics (e.g. Pluta, 1988). In contrast, charged couple device (CCD) based colour cameras coupled to a computer are capable of producing a final perceptible image in a few minutes or less. These devices, however,

often fail to capture all the spatial information that is available.

Here the means of producing colour micrographs from data sets collected with high-resolution colour CCD are described, where high resolution is defined as being in excess of  $3300 \times 2200$  pixels that each describe three (or more) completely separate channels of information which each have a potential bit depth of 8 or more. In addition, these images are compared with those produced from high quality 35 mm colour reversal photographic film.

## Methods

A Leaf Microlumina high definition ( $3380 \times 2699$  pixels total output per image data file) colour CCD camera (ISS, Greater Manchester, U.K.) was mounted on an Axiophot microscope (Zeiss, Jena, Germany) using a magnifying adapter that gave the same field of view as 35 mm film mounted in the integral camera backs of the microscope. This adapter was adjusted until the scanning plane of the camera sensor was parfocal with the internal focusing crosshair display of the Axiophot. Transmitted illumination was provided by a stabilized quartz halogen source with a fixed colour temperature of 3200 K. These emissions were subsequently filtered through Cibachrome 0.5 C and 0.1 M filters (Ilford, Cheshire, U.K.) to produce a colour balance that was better suited to the spectral response of the camera. The use of this type of illumination avoided temporal fluctuations in the intensity of the illumination whilst the image was being collected: the standard deviation of the temporal fluctuations in lines of pixels that lay along the direction in which the sensor was scanned and spanned at least 20% of the field of view was approximately one grey level in an 8 bit grey scale in each channel of colour. The 36 bit data (three channels of 12 bits each) generated by the sensor of the camera (a  $3 \times 2699$  pixel array scanned across the field of view) was truncated to the most significant 8 bits for each channel and transferred to the computer through a SCSI interface (AHA-2940, Adeptec Inc., California, U.S.A.) using proprietary software supplied with the camera which ran as

a TWAIN 32 plugin with all of the following: Adobe Photoshop (v4.0, Adobe Systems Inc., California, U.S.A.), Microsoft Photo Editor (v3.0, Microsoft Corporation Inc., Washington, U.S.A.), Corel Photopaint (v7.373, Corel Corporation, Ontario, Canada). The data were displayed on a 21-in monitor (Iiyama Electric Co. Ltd, Nagano-shi, Japan) driven by a Millenium video card (Graphics Inc., Quebec, Canada) fitted with 8 Mbyte of RAM. Data were displayed on the monitor as a matrix of up to  $1600 \times 1200$  elements in 24 bit colour, unless stated otherwise. The proprietary software used to collect data was permitted to calibrate the camera by balancing the red, green and blue channels to make an empty field of view appear a neutral grey. Following calibration, the software was used to collect image data sets using a routine that ensured that the brightest pixels were not quite saturated without generating a conflict with the balance of colours that had been determined previously. The darkest pixels in all the channels always possessed a value that was greater than zero. The orientations of the final data sets were rotated by integer multiples of  $90^\circ$  and an effectively reversible, neutral contrast stretch was performed (i.e. all the channels were treated identically so that no more than 1% of the darkest red, green and blue pixels took on a null value and 1% of the brightest pixels took on a value of 255) using Adobe Photoshop. Where required, correction of any spatial shading effects was made after two data sets had been collected, one describing a region of interest and the other a nearby empty field of view. Correction of spatial shading was implemented by dividing each pixel value in the region of interest by the equivalent pixel value in the empty field of view and multiplying the product by 250, for each of the three channels, using Image-Pro Plus (v3.0, Media Cybernetics, Maryland, U.S.A.). The resulting data set was then subjected to contrast stretching as described above. Permanent micrographs of the image data sets were made by exporting the 24 bit RGB TIFF files to a Phaser 450 dye sublimation printer (Tektronix Inc., Oregon, U.S.A.) which printed them with the printer controller software set to its bright colour setting.

Photographs of the specimens were taken on tungsten balanced colour reversal film with a stated rating of ISO64/19° (Fujichrome, Tokyo, Japan) fitted in the camera backs of the Axiophot microscope using stabilized illumination with a colour temperature of 3200 K. Exposures were restricted to a range of 0.125–2.0 s by means of neutral density filters and a range of seven exposures, at half stop intervals starting one stop below the auto-exposure reading, were collected for each field of view. The film was processed and Ciba prints hand-produced by a commercial processing company (Contour, London, U.K.). The processing company was supplied with high quality images of similar histochemical preparations to enable them to achieve an appropriate colour balance when making the reversed contrast prints. Alternatively, final images were produced by scanning regions of interest in the transparencies with

the high resolution CCD camera through the microscope fitted with a  $\times 5$  NA 0.15 objective. The presence or absence of features of interest in 35 mm photomicrographs was initially established by inspecting them with a transilluminated  $\times 6.35$ – $\times 50$  zoom MZ8 dissecting microscope (Leica, Milton Keynes, U.K.).

## Results

In order to describe the requirements of a high-resolution colour CCD camera it is necessary to define both colour and high resolution. Here colour is taken to mean photons with wavelengths that fall within the range 400–700 nm (e.g. Emsley, 1953). To utilize the capabilities of human visual perception fully under conditions of moderate to bright illumination a minimum of three channels of data, blue, green and red, must be collected. Here, when the resolution of a camera had to be calculated, extreme wavelengths of 400 (violet), 500 (blue–green) and 650 (red) nm were selected to represent these colours. These wavelengths were biased, deliberately, to describe the maximum resolution needed: more typical wavelengths would be 450 nm for the blue and 540 nm for the green. High resolution can be defined as sufficient resolution to collect all the spatial information that is available in the field of view. If the optics of a system are diffraction limited, the illumination incoherent and large numbers of photons detected (a good approximation for the microscope used here) the Rayleigh criterion suggests that two point objects can just be resolved if they are separated by a distance  $L$ , when

$$L = 0.61\lambda/NA \quad (1)$$

where  $\lambda$  is the wavelength of the light and NA the numerical aperture of the objective. Sampling theory dictates that two data points must be collected between two objects if they are to be resolved (e.g. Castleman, 1993) and combining this with Eq. (1) meant that to achieve full resolution the width of a sensor element (here a pixel in the detector),  $W$ , has to be

$$W \leq 0.61\lambda M/(2NA) \quad (2)$$

where  $M$  is the magnification of the object in the plane of the sensor.

Providing that the sensor elements completely fill the sensor, the number of sensor elements,  $N$ , then has to be

$$N \geq 3.28A \cdot NA/(\lambda M) \quad (3)$$

where  $A$  is the width of the sensor array. There are two further factors which can increase the number of sensor elements that are required, however. Firstly, with rectangular sensor elements their length is greatest along their diagonal. As an extreme example, if the sensor elements are square their density will need to be increased by a factor of  $\sqrt{2}$  to give complete sampling across the diagonal of the data set. Second, with incoherent illumination, the ability of

**Table 1.** Values of  $NA/M_{obj}$  for some typical objectives.

Magnification (×)	Numerical aperture	$NA/M_{obj}$
5	0.15	0.030
6.3	0.16	0.025
10	0.30	0.030
10	0.25	0.025
20	0.6	0.030
40	0.8	0.020
40	1.2	0.030
40	1.3	0.033
63	1.4	0.022
100	0.95	0.010
100	1.3	0.013
100	1.4	0.014

a light microscope to resolve pairs of parallel lines is better than its ability to resolve pairs of points, by a factor of  $\approx 1.22$  (e.g. Pluta, 1988). To make some allowance for these, Eq. (3) was rounded up to

$$N \geq 4A \cdot NA / (\lambda M) \tag{4a}$$

Equation (4a) is more convenient to use if the magnification is divided into the magnification of the objective,  $M_{obj}$ , and the residual magnification in the remainder of the optical path,  $M_{path}$ , giving

$$N \geq (4A/M_{path}) \cdot (1/\lambda) \cdot (NA/M_{obj}) \tag{4b}$$

Equation (4b) shows that the number of sensor elements needed was dependent upon the numerical aperture of the objective divided by its magnification. This value is normally highest for objectives of lower magnification (Table 1) and so it is with these objectives that the greatest density of pixels will usually be required. For the purposes of illustration the number of sensor elements needed when  $NA/M_{obj}$  took on values of 0.033 (e.g.  $0.33/\times 10$ ,  $1.3/\times 40$ ), 0.030 (e.g.  $0.3/\times 10$ ), 0.022 (e.g.  $1.4/\times 63$ ) and 0.014 (e.g.  $1.4/\times 100$ ) were determined. To calculate the width of the sensor it was assumed that the colour CCD camera had to have the same size of field of view as that obtained with 35 mm film. In the primary image plane of the microscope, a good reference point as  $M_{path} = 1$ , the field of view needed to be 14 mm along the longer axis. These values were substituted into Eq. (4b) and the number of sensor elements needed to give the full resolution was calculated (Table 2). This indicated that for full resolution throughout the visible spectrum, for the objectives in common use that have the highest resolution and largest field of view, presently  $\times 63$  NA 1.4 objectives, at least 3080 sensor elements were needed. They also indicated that if a sensor had in excess of 3360 elements along its long axis it would be capable of collecting almost all of the spatial

**Table 2.** The number of square CCD camera elements needed to give full resolution with a field of view equivalent to that of 35 mm colour reversal film.

$NA/M_{obj}$	Wavelength (nm)		
	400	500	650
0.0325	4550×3033	3640×2427	2800×1867
0.0300	4200×2800	3360×2240	2585×1723
0.0220	3080×2054	2464×1623	1896×1264
0.0140	1960×1307	1568×1046	1207×804

information that was available for the vast majority of objectives. Here then, the definition of a high-resolution CCD camera with the capacity of 35 mm film is taken to be a device that had the equivalent of at least 3360 sensor elements along its long axis and at least 2240 elements along its short axis. Strictly, the definition should be  $1.12 \times 10^5$   $NA/M_{obj}$  sensor elements (pixels) along the long axis of the field of view but such a definition is not particularly practical. If the CCD camera is defined as a high-resolution colour camera then this density of pixels applied to each of the three channels of data collected separately. If a colour camera was designed to collect more than three channels of data, e.g. violet, blue, green, orange, red and far red, it might be possible to reduce the number of pixels required in each channel without any loss of resolution.

When images that were generated from the data sets collected with the high-resolution colour CCD camera were compared with images prepared from colour film they were found to be directly equivalent. To illustrate the comparison between the use of a high-resolution CCD camera and slow colour reversal film the cross striations in a preparation of skeletal muscle were examined. The repeating interval of the linear cross striations themselves was about  $3 \mu\text{m}$ , which should be resolved clearly by an NA 0.15 objective but not by an NA 0.075 objective (e.g. Pluta, 1988). Within the cross striations the linear Z bands lay about 825 nm from the A band and these should be resolved with an NA 0.5 objective but not an NA 0.3 objective (e.g. Pluta, 1988). When either slow colour reversal film or the high-resolution CCD camera was used the cross striations in a preparation of skeletal muscle cells were visible when a  $\times 5$  NA 0.15 objective was used (Fig. 1A and B, respectively) but not when a  $\times 2.5$  NA 0.075 objective was employed (data not presented). Similarly, in intensely stained regions of the skeletal muscle the Z band was just apparent in images reproduced from slow colour reversal film and the data sets collected with the high resolution colour CCD camera when a  $\times 20$  NA 0.5 objective was used (Fig. 1C and D,

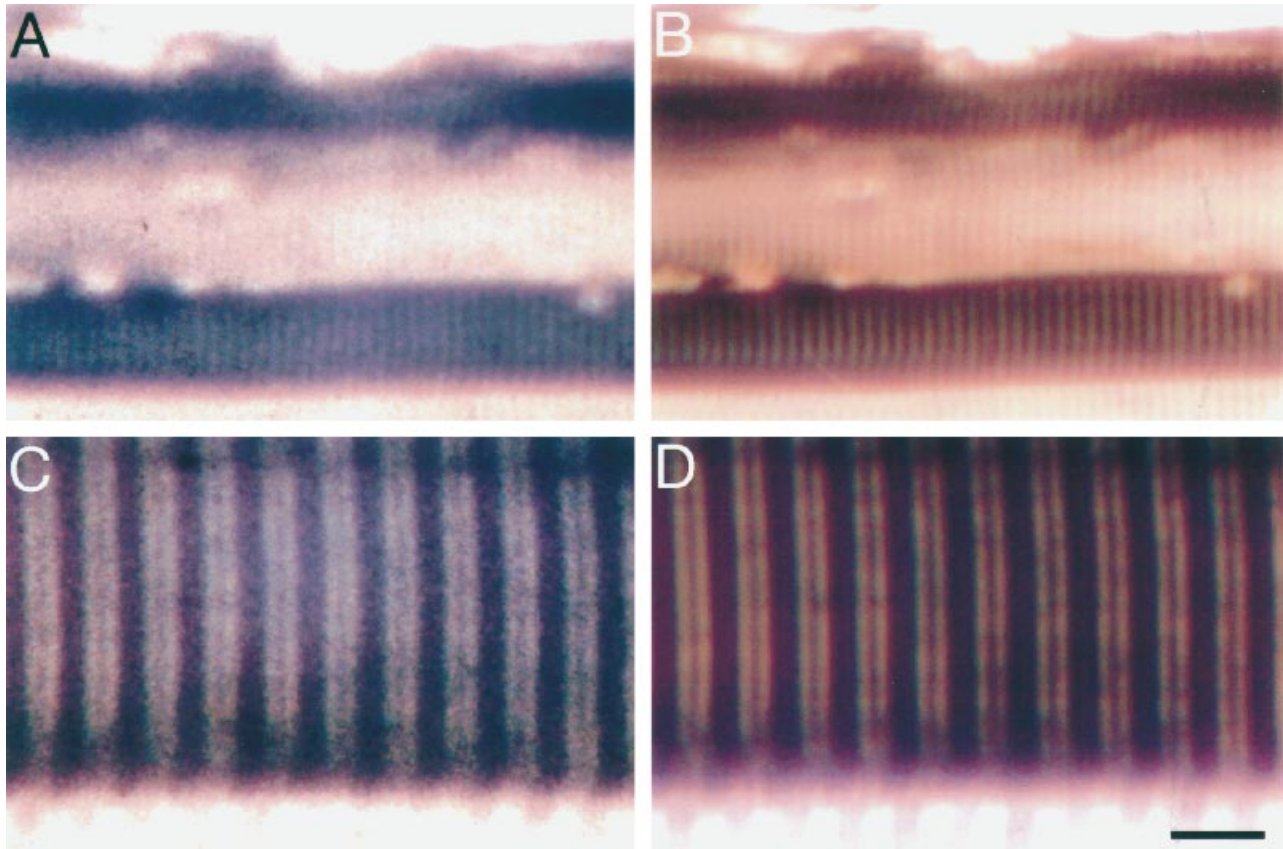


**Fig. 1.** Mammalian skeletal muscle sectioned and stained with iron haematoxylin. Images were captured on Fujichrome tungsten balanced colour reversal film with a stated rating of ISO64/19° (A, C) and images created from data generated by the high-resolution colour CCD camera (B, D). The scale bar represents, 20  $\mu\text{m}$  (A, B), 5  $\mu\text{m}$  (C, D).

respectively) but was not apparent when a  $\times 10$  NA 0.3 objective was used (data not presented). The muscle was not stretched sufficiently to make the two parts of the A bands appear as discrete entities with the  $\times 20$  NA 0.5 objective in all but the most lightly stained tissue. Some noise was apparent in the final figures prepared from the images captured on colour reversal film (Fig. 1A and C) which was due to the individual grains of silver in the film ( $\approx 100$  nm length) becoming visible in the final image. Finally, when preparing the final figure parts from primary images captured on colour reversal film the contrast achieved was higher when the regions of interest in the transparencies were scanned with the high-resolution CCD camera and the data sets printed with the dye sublimation printer than when highly enlarged reverse contrast prints (Ciba prints) were made directly from the transparencies. Consequently, the final figures were prepared from image data sets that recorded scans of the transparencies. The superior performance of the CCD camera over conventional methods of printing film was not especially surprising. Firstly, the colour reversal film was scanned using a  $\times 5$  NA 0.15 objective that massively oversampled the regions of interest

in the transparencies such that individual silver grains were easily recognized. Secondly, the CCD camera possessed a much higher colour contrast sensitivity than film (see below).

When film is used, the process of collecting an image as a transparency and the printing of the final figure is usually carried out without significant loss of information. In contrast, with a high-resolution colour CCD camera the entire data set cannot be presented on a single computer monitor screen simultaneously, at least not with the monitors that are readily available at present. In order to visualize the full field of view the data must be compressed spatially either by averaging the values for a number of adjacent pixels or by discarding some pixel values. Alternatively, the full resolution of the camera can be displayed, but only for a part of the field of view. For example, when skeletal muscle was visualized with a  $\times 5$  NA 0.15 objective the fainter cross-striations were only apparent if each pixel of data occupied a  $2 \times 2$  matrix of pixels in the display on the computer monitor screen. This consideration restricted the field of view to a matrix of  $800 \times 600$  pixels. Moreover, most observers found that the quality of the images found in

these displays was equivalent to that found when the full field of view collected with a  $\times 0\text{NA } 0\cdot6$  objective was displayed (10/10 observers). In general, photomicrographs should show the largest possible field of view that is consistent with the accurate representation of the smallest objects of interest; this maximizes the number of interesting objects that can be displayed. Having selected the appropriate magnification the data should then be collected with as much definition as possible, i.e. by using the largest practical numerical aperture. Combining these two considerations with the observations described above indicated that there was little information in data sets collected with a  $\times 20\text{NA } 0\cdot6$  objective that could not either be made readily visible in an equivalent data set collected with a  $\times 5\text{NA } 0\cdot15$  objective or sampled more effectively with a  $\times 40\text{NA } 0\cdot75$  objective. Consequently, at least when the light microscope was used to examine histologically stained preparations, a single data set that described a relatively large field of view together with a series of data sets that described specific features of interest taken with an eight-fold increase in magnification were sufficient to describe the salient points completely.

When data are transformed into an image by means of a dye sublimation printer, or other computer linked printing device, the size of the final image can be very large indeed. In the context of scientific publications, however, the usual upper bound is slightly smaller than standard A4 in size (177  $\times$  226 mm in the case of the *Journal of Microscopy*) and for a single plate in a multi-part figure a typical value is 84  $\times$  56 mm (e.g. Fig. 1). In consequence, the number of pixels that can be reproduced usefully from an image data set is an important issue. In order to study this, parts of Fig. 1 and similar figures reproduced at different sizes were inspected by a number of, generally young (<25 years.), observers (20) who all held the printed images  $\approx 250$  mm from their eyes. It was found that to depict fine detail accurately the width of the pixels had to subtend an angle of 2.4–7.3 seconds of arc at the eye of the observer (equivalent to  $\approx 50$ –150 dots per inch). Hence, to enable the general reader, as opposed to the average observer, to see all the details in an average image the width of the pixels had to subtend an angle of at least 5 seconds of arc (equivalent to  $\approx 100$  dots per inch). To print some low contrast images that described fine details with an inherently low contrast (e.g. Fig. 1), lower densities of pixels were required. Consequently, each case was decided upon its merits. In general, however, when the width of the pixels subtended an angle of 5 seconds of arc at the eye of the observer (equivalent to  $\approx 100$  dots per inch) reproductions of the relevant parts of data sets collected with a  $\times 5\text{NA } 0\cdot15$  objective were equivalent in quality to reproductions of the full field of view collected with a  $\times 20$  objective, unless very large images were produced (Table 3).

Different views taken from a single data set reproduced

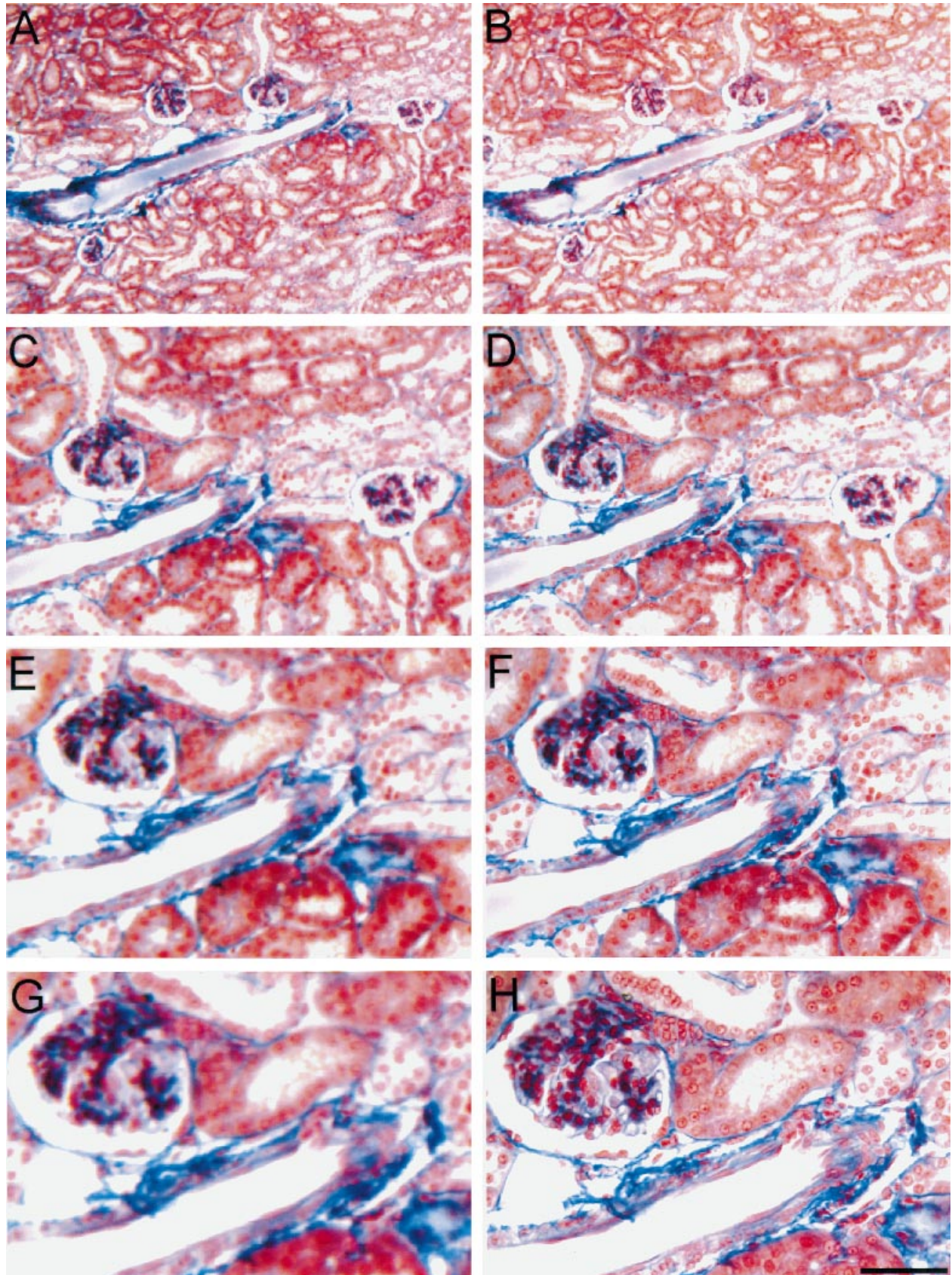
**Table 3.** The magnification of an objective whose full field of view can be emulated successfully using the data collected with a  $\times 5\text{NA } 0\cdot15$  objective in a printed reproduction.

Printing density (d.p.i.)	Size of final image (mm)		
	226 x 177 (A4)	177 x 118	84 x 56
50	$\times 30$	$\times 40$	$\times 80$
100	$\times 15$	$\times 20$	$\times 40$
150	$\times 10$	$\times 15$	$\times 30$

with pixel widths that subtended an angle of 5 seconds of arc (equivalent to  $\approx 100$  dots per inch) were adequate to describe a  $\times 6$  to  $\times 9$  fold range of magnifications. Fields of view were extracted from a single data set collected with a  $\times 5$  objective that corresponded to the same area found in one half of the full field of view collected with a  $\times 10$ , a  $\times 20$  and a  $\times 40$  objective (Fig. 2). These images were equivalent to the full field of view that would have been obtained with a  $\times 15$ , a  $\times 30$  and a  $\times 60$  objective, respectively. A view that corresponded to the full field of view that would have been obtained with a  $\times 45$  objective was also included for completeness (Fig. 2E and F). The images generated from the data set collected with the  $\times 5\text{NA } 0\cdot15$  objective were very similar to those obtained at objective magnifications of  $\times 15$  and  $\times 30$  (Fig. 2 compare parts A and B and parts C and D). The very fine structure of the tissue became more visible only when images depicting the full field of view at  $\times 45$  were compared with the appropriate part of the data set collected with the  $\times 5\text{NA } 0\cdot15$  objective. Even here, displaying the equivalent portion of a data set collected with the  $\times 5$  objective was an adequate substitute for the reproduction of the full field of view collected at  $\times 45$  (Fig. 2 compare parts E and F). When specimens of a good quality were examined, displays of details taken from the data sets generated with the  $\times 5$  objective were not an adequate substitute for reproductions of the full field of view collected with an objective magnification of  $\times 60$  (Fig. 2G and H). If specimens were not completely flat, however, the amount of detail that could be reproduced from data sets collected using the  $\times 5\text{NA } 0\cdot15$  objective was almost identical to that reproduced from data sets collected with the  $\times 10\text{NA } 0\cdot3$ ,  $\times 20\text{NA } 0\cdot6$  and even  $\times 40\text{NA } 0\cdot75$  objectives (e.g. Fig. 3). The advantages of the deeper field of view collected with the lower NA objectives were also apparent when thick specimens were examined (data not presented).

When the slight unevenness of the illumination was corrected for and the contrast in the resulting data set expanded to fill the complete range that was available, the high-resolution colour CCD camera exhibited a very high sensitivity to contrast. A tumour of the submaxillary gland







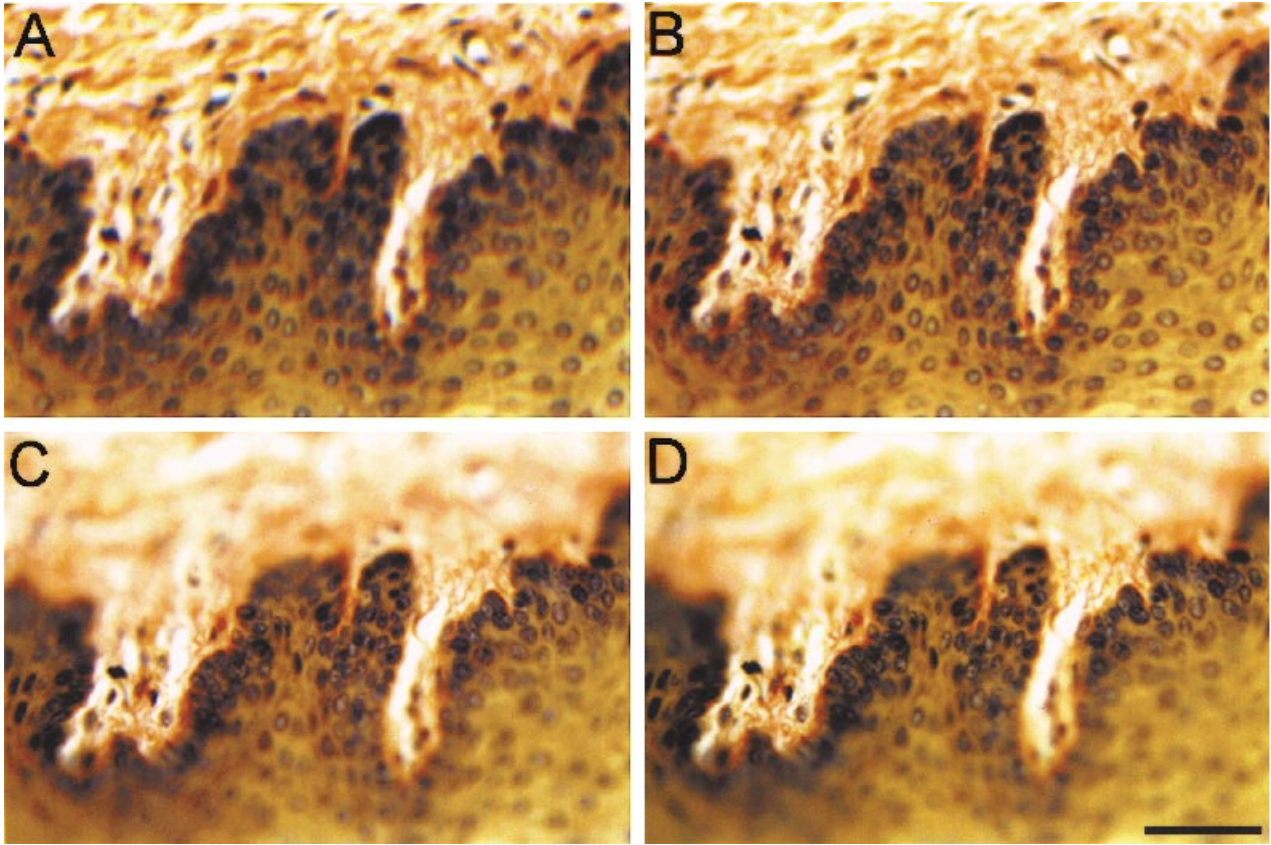


**Fig. 3.** Mammalian tongue sectioned and stained with iron haematoxylin and van Gieson's stain. Image data sets were collected with the CCD camera and the following air objectives:  $\times 5$  NA 0.15 (A),  $\times 10$  NA 0.3 (B),  $\times 20$  NA 0.6 (C) and a  $\times 40$  NA 0.8 (D) objective. The scale bar represents  $50\ \mu\text{m}$ .

in a transgenic mouse carrying a lacZ reporter gene was treated to reveal the expression of  $\beta$ -galactosidase using the chromogenic substrate 4-chloro, 5-bromo, 3-iodolyl  $\beta$ -galactosidase. After staining, the tumour exhibited a distinctly blue hue. When the tissue was sectioned, however, the regions of staining were virtually imperceptible even after considerable contrast stretching (Fig. 4A and B). When the maximum degree of reversible contrast stretching (see Methods) was applied to the data set, blue staining became clearly visible in the sections (Fig. 4C). Here, however, interpretation of the data was made difficult by the presence of artefacts that were obviously due to shading effects, which the contrast stretching also magnified greatly. When a shading correction was applied to the data set (see Methods) the perception of the blue staining was improved

very markedly without the generation of the artefacts (Fig. 4D). The pink coloration of the tissue not expressing lacZ was entirely expected, as tissue or any other material whose lack of transparency is largely due to Rayleigh scattering of light, scatters blue light far more efficiently than it scatters red light.

### Discussion

Providing that the density of the elements found on the long axis of a sensor is high enough ( $1.12 \times 10^5$  NA/ $M_{\text{obj}}$  for each of the three channels of information; blue, green and red) the resolution achieved with a colour CCD camera equals that obtained with fine grained 35 mm colour film over an equivalent field of view. To ensure that the results of

**Fig. 2.** A comparison of pairs of images of the cortex of mammalian kidney obtained with objectives of different magnifications and numerical apertures. After sectioning, the tissue was stained with Azan triple stain. Image data sets were collected by the CCD camera and the following air objectives:  $\times 5$  NA 0.15 (A, C, E, G),  $\times 10$  NA 0.3 (B),  $\times 20$  NA 0.6 (D, F) and  $\times 40$  NA 0.8 (H). The scale bar represents,  $200\ \mu\text{m}$  (A, B),  $100\ \mu\text{m}$  (C, D),  $67\ \mu\text{m}$  (E, F),  $50\ \mu\text{m}$  (G, H).

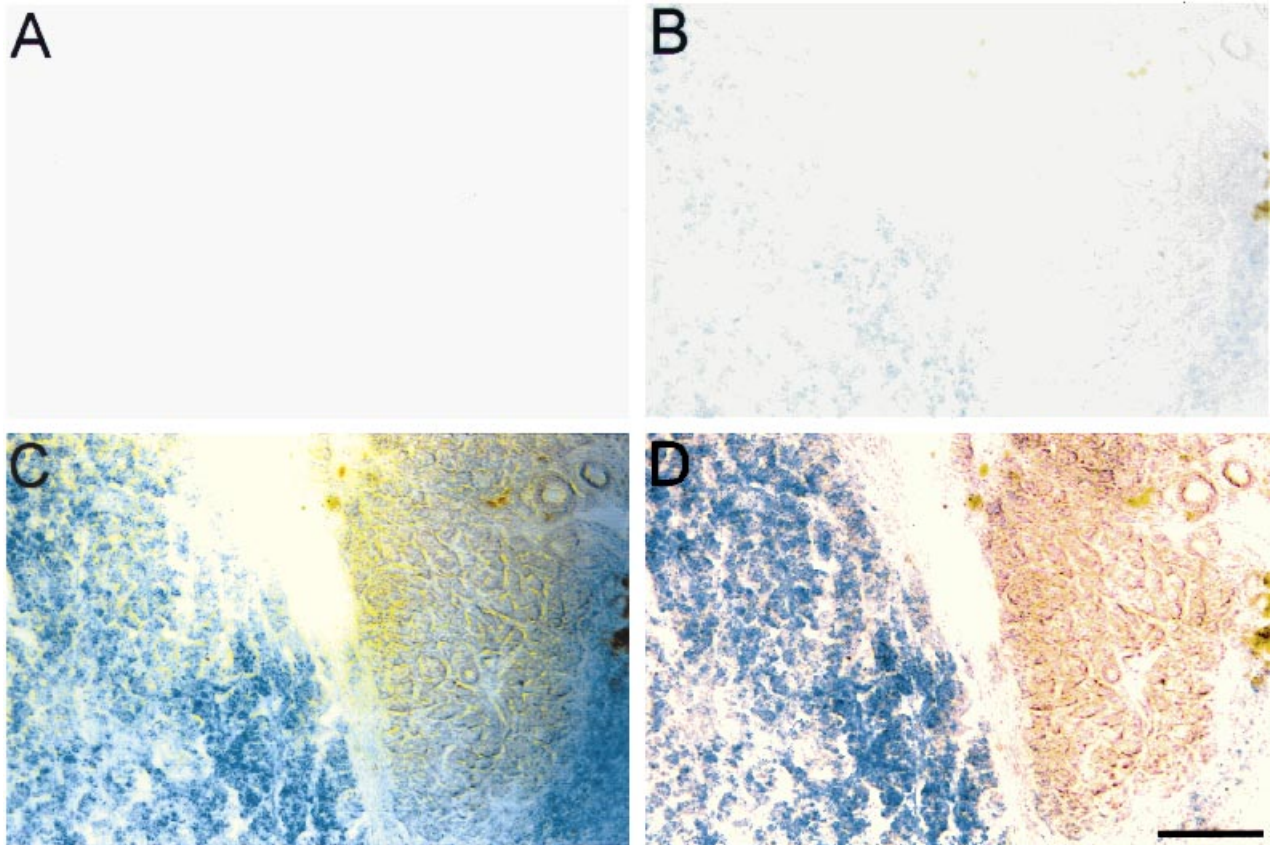


**Fig. 4.**  $\beta$ -Galactosidase activity in a section of murine submaxillary tumour. A data set collected with the CCD camera depicting the original data set (A); similar images after the application of a four-fold contrast stretch to the data set (B), an eight-fold contrast stretch to the data set (C); an image of the data set after the application of a correction for shading and an eight-fold contrast stretch (D). The scale bar represents 125  $\mu$ m.

this study were applicable to all objectives, those that had a high numerical aperture to magnification ratio were used wherever practical (Tables 1 and 2). This meant that most of the specimens were viewed with low powered objectives, e.g.  $\times 5$  NA 0.15 or a  $\times 10$  NA 0.3. All of the observations and comments made here, however, apply equally to objectives of high magnification and numerical aperture.

The contrast that can be extracted from the data sets collected with a high-resolution colour CCD camera far exceeds that obtainable from colour film. Moreover, when additional compensation is made for any shading introduced by the components of the microscope, the contrast sensitivity of colour CCD cameras exceeds that of human vision. The process used to correct the shading artefacts is not entirely new as it is the digital equivalent of the well-known analogue video enhanced contrast techniques (Allen *et al.*, 1981a,b; Inoué, 1981).

The density of information collected by a high-resolution CCD camera is such that part or all of the data describing specimens can be displayed, usefully, on both computer monitor screens and the printed page over a four-fold range

of magnification. Moreover, with difficult specimens, such as those that are distorted or very thick, the range of magnification over which the data, or details taken from the data sets, can be shown is closer to eight-fold. Coupling this potential for zooming in on regions of interest with the ease of duplication and retrieval of computer image data files has important implications in any branch of light microscopy that involves recording images of specimens for archival or training purposes, e.g. with specimens depicting healthy and diseased tissues. To make progress on this front will, however, require that satisfactory methods of compressing the 26.1 Mbyte data files are found.

#### Acknowledgements

I would like to thank my family and those colleagues at the Ludwig Institute for Cancer Research who patiently inspected and compared figures. I also wish to thank the following for supplying specimens: Katrin Bussell and Alastair Reith of the University College London Branch of the Ludwig Institute for Cancer Research (LICR) for



providing the murine tumour material and Mike O'Hare of the Ludwig Institute for Cancer Research and University College London, Breast Cancer Laboratory (Department of Surgery, London) for providing the sections of skeletal muscle, kidney and tongue. Finally, I would like to thank Mike O'Hare and Anne Ridley (LICR UCL branch) for helpful comments on the preparation of this manuscript.

### References

- Allen, R.D., Allen, N.S. & Travis, J.L. (1981a) Video-enhanced contrast differential interference contrast (AVEC-DIC) microscopy. A new method capable of analyzing microtubule-related motility in the reticulopodial network of *Allogromia laticollaris*. *Cell Motility*, **1**, 291–302.
- Allen, R.D., Travis, J.L., Allen, N.S. & Yilmaz, H. (1981b) Video-enhanced contrast polarisation (AVEC-POL) microscopy. A new method applied to the detection of birefringence in the motile reticulopodial network of *Allogromia laticollaris*. *Cell Motility*, **1**, 275–288.
- Castleman, K.R. (1993) Resolution and sampling requirements for digital image processing, analysis and display. *Electronic Light Microscopy* (ed. by D. Shotton), pp. 71–93. Wiley-Liss, New York.
- Emsley, H.H. (1953) *Visual Optics* Vol. II *Physiology of Vision*, pp. 216–233. Butterworth, London.
- Inoué, S. (1981) Video image processing greatly enhances quality and speed in polarisation based microscopy. *J. Cell Biol.* **89**, 346–356.
- Pluta, M. (1988) *Advanced Light Microscopy* Vol. 1: *Principles and Basic Properties*, pp. 285–373. Elsevier, Amsterdam.